Paull, C.K., Matsumoto, R., Wallace, P.J., and Dillon, W.P. (Eds.), 2000
Proceedings of the Ocean Drilling Program, Scientific Results, Vol. 164

36. THE GEOMICROBIOLOGY OF DEEP MARINE SEDIMENTS FROM BLAKE RIDGE CONTAINING METHANE HYDRATE (SITES 994, 995, AND 997)[1]

Peter Wellsbury,[2] Kim Goodman,[2] Barry A. Cragg,[2] and R. John Parkes[2]

ABSTRACT

Bacterial populations and activity were quantified at three sites on the Blake Ridge, Ocean Drilling Program Leg 164, which formed a transect from a point where no bottom-simulating reflector (BSR) was present to an area where a well-developed BSR existed. In near-surface sediments (top ~10 mbsf) at Sites 994 and 995, bacterial profiles were similar to previously studied deep-sea sites, with bacterial populations (total and dividing bacteria, viable bacteria, and growth rates [thymidine incorporation]) highest in surface sediments and decreasing exponentially with depth. The presence of methane hydrate was inferred at depth (~190–450 mbsf) within the sediment at all three sites. Associated with these deposits were high concentrations of free methane beneath the inferred base of the hydrate. Bacteria were present in all samples analyzed, to a maximum of 750 mbsf, extending the previous known limit of the deep biosphere in marine sediments by ~100 m. Even at this depth, the population was substantial, at 1.8×10^6 cells mL^{-1}. Bacterial populations and numbers of dividing and divided cells were stimulated significantly below the base of the inferred hydrate zone, which may reflect high concentrations of free gas. Localized increases in bacterial populations within the hydrate stability zone may also have been associated with free gas. Solid methane hydrate, recovered from 331 mbsf at Site 997, contained only 2% of the predicted bacterial population in a sediment from this depth, suggesting reduced bacterial populations in solid hydrate.

Bacterial activity in near-surface sediments was dominated by sulfate reduction. Sulfate reduction rates and pore-water sulfate decreased rapidly with depth, concomitant with an accumulation of solid-phase sulfide in the sediment. Once sulfate was depleted (~20–30 mbsf), methane concentrations, methanogenesis, and methane oxidation all increased. Below 100 mbsf, bacterial processes occurred at very low rates. However, bacterial activity increased sharply around 450 mbsf, associated with the base of the inferred hydrate zone and the free-gas zone beneath; anaerobic methane oxidation, methanogenesis from both acetate and H_2:CO_2, acetate oxidation, sulfate reduction, and bacterial productivity were all stimulated (from 1.5 to 15 times), demonstrating that the sediments near and below the BSR form a biogeochemically dynamic zone, with carbon cycling occurring through methane, acetate, and carbon dioxide. At Site 995, pore-water acetate was present in surprisingly high concentrations, reaching ~15 mM at 691 mbsf, ~1000 times higher than "typical" near-surface concentrations (2–20 μM). Potential rates of acetate metabolism were extremely high and could not be sustained without influx of organic carbon into the sediment; hence in situ rates are likely to be lower than these potential rate measurements. However, there is evidence for upward migration of high concentrations of dissolved organic carbon into the sediments at these sites.

Rates of acetate methanogenesis below the BSR were 2–3 orders of magnitude higher than H_2:CO_2 methanogenesis and were associated with extremely high quantities of free gas. Methane oxidation rates at the base of the hydrate zone at Site 995 were 10 times greater than H_2:CO_2 methanogenesis. However, acetate methanogenesis at Site 995 exceeded methane oxidation through and below the BSR, potentially providing an unexpected source of methane gas for the formation of hydrates. These results confirm and extend previous results from Cascadia Margin, demonstrating that gas hydrate–containing sediments provide a unique deep bacterial habitat in marine sediments.

INTRODUCTION

Gas hydrates form under conditions of low temperature, high pressure, and an adequate supply of gas (usually methane). Global methane hydrate deposits in sediments are estimated to contain ~10^4 Gt of carbon, approximately twice that estimated for all other global fossil fuel deposits (Kvenvolden, 1988). In addition, the solid hydrate strata may act as a seal, resulting in the accumulation of considerable volumes of free gas below the bottom-simulating reflector (BSR). Methane is a potentially significant energy source for bacteria; thus, gas hydrates may provide a globally significant energy source for deep sediment bacteria in marine environments.

Previous investigation into microbial activity in gas hydrate–bearing sediments in the Cascadia Margin (Ocean Drilling Program [ODP] Leg 146) demonstrated that both bacterial populations and their activity increased significantly in association with the presence of a discrete zone of gas hydrate, such that within the hydrate zone deep bacterial activity was greater than at the sediment surface (Cragg et al., 1995). Rates of anaerobic methane oxidation increased in a discrete hydrate zone (Site 889/890) to approximately nine times the rate at other depths, coincident with an order of magnitude increase in the total bacterial population. However, rates of bacterial methanogenesis from H_2:CO_2 were five orders of magnitude lower than oxidation rates (Cragg et al., 1996), suggesting either a significant local flow of methane into the sediment or a source of methane in addition to H_2:CO_2 methanogenesis.

ODP Leg 164 was dedicated to improving knowledge of the in situ characteristics and amounts of natural gas hydrates in sediments, via a drilling regime at three sites (Sites 994, 995, and 997) on the Blake Ridge to 750 m depths, which included drilling through the hydrate-stability field and the BSR and into the sediments below. In Blake Ridge sediments, the bulk (98%+) of gas in the hydrates is methane, and isotopic and compositional data indicate a microbial origin (Brooks et al., 1983; Galimov and Kvenvolden, 1983). Thus, Leg 164 offered an opportunity (1) to demonstrate whether the results from Leg 146 were representative of other gas hydrate sites, (2) to investigate further the importance of deep bacterial processes for driv-

[1]Paull, C.K., Matsumoto, R., Wallace, P.J., and Dillon, W.P. (Eds.), 2000. *Proc. ODP, Sci. Results,* 164: College Station, TX (Ocean Drilling Program).

[2]Department of Earth Sciences, University of Bristol, Wills Memorial Building, Queens Road, Bristol BS8 1RJ, United Kingdom. Correspondence author: peter.wellsbury@bristol.ac.uk

ing geochemical changes, and (3) to investigate the origin of methane in the gas hydrate deposits.

MATERIALS AND METHODS

Site Description

Samples for determination of bacterial populations and activity were taken from cores at three sites on the Blake Ridge (Paull, Matsumoto, Wallace, et al., 1996). These sites (Sites 994, 995, and 997) formed a transect from an area on the southern flank of the Blake Ridge where a BSR was not detectable to an area where an extremely well-developed BSR existed (Fig. 1).

No BSR was observed at Site 994, and thus Site 994 was originally intended as a control site without gas hydrates but with the same sediment types. However, downhole interstitial water chloride anomalies, temperature anomalies in recovered cores, and patterns in the downhole log data indicated that gas hydrates were present in the sediment, typically occupying between 1 and 3 vol% of the sediments between 220 and 430 mbsf, with several intervals containing up to 9.5% gas hydrate.

At Site 995 a modest BSR was detected (Fig. 1), and the interstitial water geochemistry and physical properties were very similar to those at Site 994. Although no gas hydrate was recovered from Site 995, downhole interstitial water chloride anomalies, anomalies in recovered core temperatures, and patterns in the downhole log data indicated that gas hydrates occupied between 1 and 4 vol% of the sediments between 195 and 450 mbsf, with several intervals containing up to 10% gas hydrate. The BSR was apparently associated with the first occurrence of free gas.

Site 997 was located on the topographic crest of the Blake Ridge, and possesses an extremely well-developed and distinct BSR. Interstitial water chloride anomalies, temperature anomalies in the recovered cores, and patterns in the downhole log data indicated that gas hydrate occupies between >1.5 and 4 vol% or more of the sediment from 195 to 450 mbsf. Several intervals contained as much as 11% gas hydrate. The BSR was associated with a zone of free gas, which was well developed for 30 m and extended for over 100 m below the BSR.

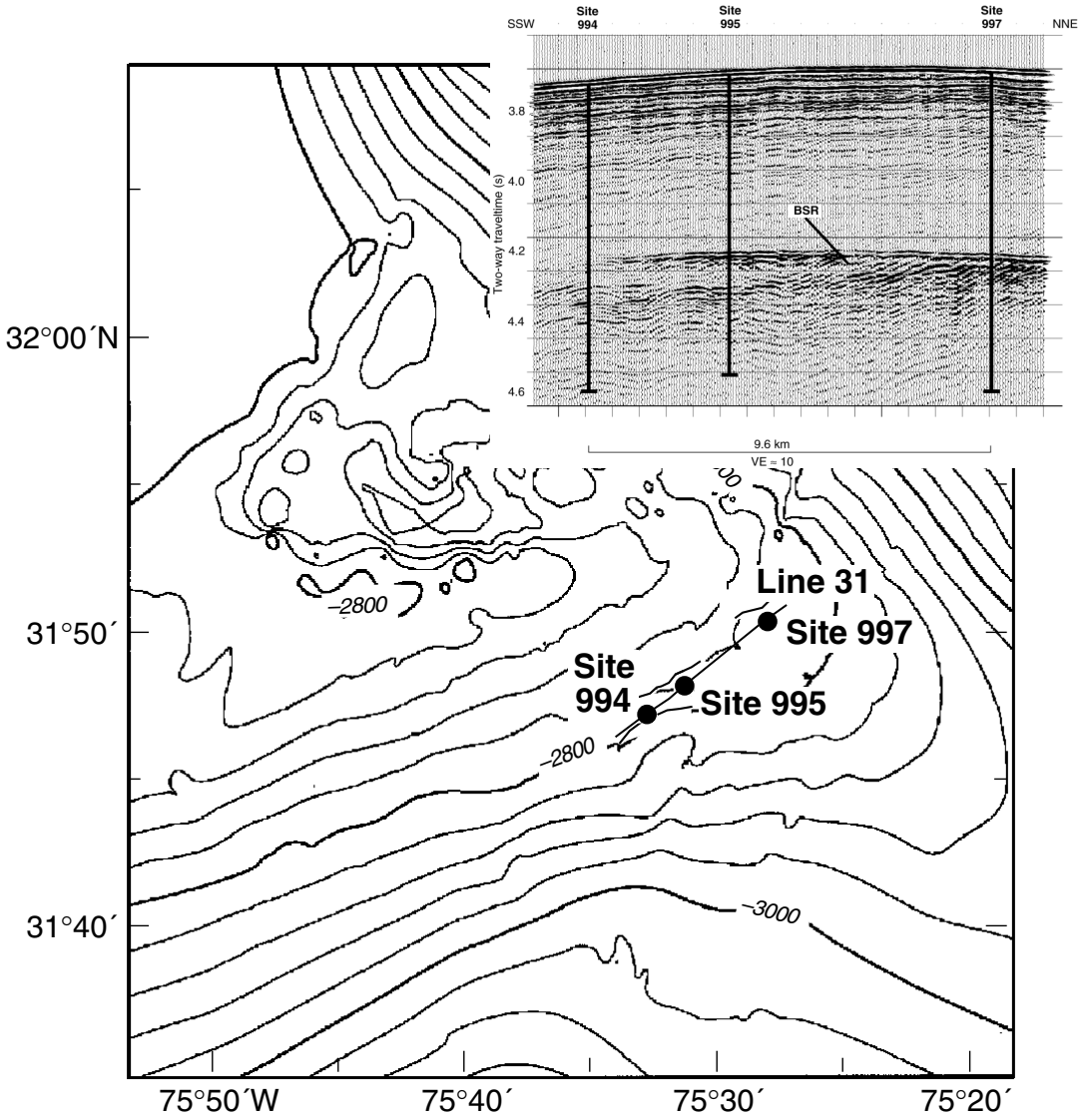

Figure 1. Blake Ridge, showing the location of Sites 994, 995, and 997 along a transect from an area with no BSR (Site 994) to a well-developed BSR (Site 997) and (inset) seismic profile along the transect line.

During Leg 164 the pressure core sampler (PCS) was deployed to allow samples of gassy sediment to be recovered at in situ pressure, releasing the gas in controlled laboratory conditions at the surface to allow accurate determination of gas quantity and composition. Results from the PCS indicated that substantial quantities of methane (~15 GT of carbon) existed in the form of solid gas hydrate at Blake Ridge (Dickens et al., 1997), and, equally important, that an equivalent or greater amount of free gas existed below the BSR.

Shipboard Sample Handling

Whole-Round Cores

All samples for measurement of potential bacterial activity and estimation of bacterial numbers were taken from either 20- or 25-cm-long whole-round cores (WRC). In total, 37 samples were obtained from Site 994 (15 × 20 cm samples, 0.1–40.81 mbsf), Site 995 (16 × 25 cm samples, 0.13–0.6 mbsf) and Site 997 (6 × 20 cm samples, 330.69–491.53 mbsf). The samples were taken from 1.5-m core sections using a specially constructed cutting rig (Parkes et al., 1995). The cut ends of the WRC were capped with sterile core end caps under a flow of sterile oxygen-free nitrogen (OFN) to maintain anaerobic conditions. Modified core end caps fitted with a one-way gas release valve were used for WRC samples containing gas hydrate to allow gas pressure to vent from the samples. Capped WRC were stored in gas-tight anaerobic bags (Cragg et al., 1992) in the ship's cold room at 4°C and transported by air back to the laboratory in insulated trunks containing wet ice and ice packs. The samples remained cold throughout transportation.

Direct Bacterial Enumeration

For direct determination of bacterial numbers, 1-cm^3 sediment samples were taken from the end of selected 1.5-m core sections immediately after the sections were cut on the catwalk. A thin layer of potentially contaminated sediment was removed from the core using a sterile scalpel. A 1-cm^3 sample was then removed using a sterile (autoclaved) 5-mL syringe from which the luer end had been removed. The sample was ejected directly into a preweighed serum vial containing 9 mL of filter-sterilized (0.2 µm) 4% (v/v) formaldehyde in artificial seawater. Additionally, three samples of "pure hydrate" were taken from the massive gas hydrate deposit at Site 997 (331 mbsf), washed with filter-sterilized (0.1 µm) water to remove external sediment and stored in capped serum vials as before, allowing gas pressure to vent through a sterile needle.

Pore Waters

Pore-water samples were filter sterilized (0.1 µm) and stored, frozen, in 2.5-mL capped vials before transportation back to the laboratory for determination of acetate concentrations by high performance liquid chromatography (HPLC).

Laboratory Sample Handling

Whole-Round Cores

On arrival at the laboratory in Bristol the WRC samples were stored in a constant-temperature room at 4°C prior to further handling. All samples were processed within three weeks of arrival.

All sample handling was performed under aseptic, anaerobic conditions (Parkes et al., 1995). WRC were cut into 5-cm sections, from each of which ten 5-cm^3 syringe subcores were removed for radiotracer potential activity measurements, and one 5-cm^3 syringe subcore for most probable number (MPN) viable counts. Syringe subcores were taken from the center of the WRC, avoiding sediment near the core liner to avoid the possibility of contamination.

The 20-cm WRC from Sites 994 and 997 were sliced into four 5-cm sections as described above, and potential rates of (1) methanogenesis from bicarbonate, (2) sulfate reduction, (3) methane oxidation and (4) thymidine incorporation were determined. Additionally, at Site 995, the fifth 5-cm section was used to determine rates of acetate turnover.

Direct Microscopy

Total numbers of bacteria were determined using acridine orange staining and epifluorescence microscopy (Fry, 1988; Fry, 1990). Formaldehyde-fixed samples were vortex mixed, and 5 µL was added to 10 mL of 2% filter-sterilized (0.1-µm filter) formaldehyde, along with 50 µL of filter-sterilized, 1 g L^{-1} acridine orange solution. After 3 min incubation, the solution was filtered through a 25-mm Nucleopore (0.2-µm pore size) black polycarbonate membrane (Costar, UK), which was rinsed with a further 10 mL of 2% filter-sterilized (0.1-µm filter) formaldehyde and mounted on a glass slide in a minimal amount of paraffin oil under a cover slip.

Mounted membranes were viewed under epifluorescent illumination (Zeiss Axioscop, 50W mercury vapor lamp, blue excitation, 100× Plan Neofluor oil-immersion objective, and 10x eyepiece). Fluorescent bacteria were enumerated; cells were recorded as "on" or "off" particles, doubling the number of cells on particles in the final calculations to account for masking. Dividing cells (with a clear invagination) and divided cells (pairs of cells with identical morphology) were also counted. Triplicate membranes were prepared and counted for each sample, with a minimum number of 200 fields of view examined for each membrane. Where replicate $\log_{10}$ counts differed by more than 0.5, a fourth membrane was prepared. This gives a detection limit of 1×10^5 cells mL^{-1} (Cragg and Parkes, 1994). Periodic blank membranes were also counted to check for potential contamination.

Enumeration of Viable Bacteria

A most probable number (MPN) technique (Hurley and Roscoe, 1983) was used to estimate numbers of viable fermentative heterotrophs; nitrate- and sulfate-reducing bacteria; and methane-oxidizing, sulfate-reducing bacteria. This procedure involved 9–11 dilution levels from the original sediment, descending serially in quadruplicate one in five dilutions. All MPN enrichments were performed in 7-mL serum vials of anaerobic media, sealed with butyl rubber septa and aluminum crimp tops (Phase Separations Ltd., Deeside, UK). Compositions of the growth media were as follows:

Fermentative heterotroph medium: 0.2 g L^{-1} KH_2PO_4; 0.25 g L^{-1} NH_4Cl; 30.0 g L^{-1} NaCl; 6.0 g L^{-1} $MgCl_2 \cdot 6H_2O$; 0.5 g L^{-1} KCl; 0.15 g $CaCl_2 \cdot 2H_2O$; 1.0 mg L^{-1} Resazurin; 0.5 g L^{-1} casamino acids; 0.1 g L^{-1} yeast extract. The pH was adjusted to 7.5 with NaOH and the medium autoclaved. Once autoclaved, the following were added from sterile, stock solutions: 3.0 mL L^{-1} of "Combined Vitamin Solution" (40.0 mg L^{-1} 4-aminobenzoic acid; 10.0 mg L^{-1} D[+] biotin; 100.0 mg L^{-1} thiamine-HCl; 20.0 mg L^{-1} folic acid; 100.0 mg L^{-1} pyridoxine-HCl; 50.0 mg L^{-1} riboflavin; 50.0 mg L^{-1} nicotinic acid; 50.0 mg L^{-1} DL calcium pantothenate; 50.0 mg L^{-1} lipoic acid; 50.0 mg L^{-1} cyanocobalmine); 3.0 mL L^{-1} of "Trace Elements 1" (190.0 mg L^{-1} $CoCl_2 \cdot 6H_2O$; 100.0 mg L^{-1} $MnCl_2 \cdot 4H_2O$; 70.0 mg L^{-1} $ZnCl_2$; 62.0 mg L^{-1} H_3BO_3; 36.0 mg L^{-1} $Na_2MoO_4 \cdot 2H_2O$; 24.0 mg L^{-1} $NiCl_2 \cdot 6H_2O$; 17.0 mg L^{-1} $CuCl_2 \cdot 2H_2O$; 1.5 g L^{-1} $FeCl_2 \cdot 4H_2O$ [dissolved first in 10 mL 25% {v/v} HCl]); 3.0 mL L^{-1} of selenite/tungstate (3.0 mg L^{-1} $NaSeO_3 \cdot 5H_2O$; 4.0 mg L^{-1} $NaWO_4 \cdot 2H_2O$); 30.0 mL L^{-1} of 84.0 g L^{-1} saturated $NaHCO_3$ solution, 3.0 mL L^{-1} of 12.0 g L^{-1} Na_2S solution; 10.0 mL L^{-1} of a mixed solution of 0.5 g glucose and 0.49 g glycerol in 10 mL water. The pH of the medium was readjusted to 7.5 and dispensed under a N_2:CO_2 headspace into sterile 7-mL vials containing 2.5 mg chitin and 2.5 mg cellulose. Each vial was sealed with a butyl rubber septum and aluminum crimp top. Positive growth in each of the vials was determined by phase-contrast microscopy.

Nitrate-reducing bacteria medium: 25.0 g L^{-1} Nutrient Broth No. 2 (Merck UK); 1.01 g L^{-1} KNO_3; 1.0 mg L^{-1} Resazurin; 25.8 g L^{-1} NaCl; 5.2 g L^{-1} $MgCl_2 \cdot 6H_2O$. The pH was adjusted to 7.5 with NaOH, and the medium autoclaved and dispensed under OFN. Positive growth in each of the vials was determined by presumptive color change (orange to yellow).

Sulfate-reducing bacteria medium: 0.5 g L^{-1} KH_2PO_4; 1.0 g L^{-1} NH_4Cl; 1.0 g L^{-1} $CaSO_4$; 2.0 g L^{-1} $MgSO_4 \cdot 7H_2O$; 0.875 g L^{-1} sodium lactate; 0.45 g L^{-1} sodium acetate; 0.1 g L yeast extract; 0.1 g L^{-1} ascorbic acid; 0.1 g L^{-1} thioglycollic acid; 0.5 g L^{-1} $FeSO_4 \cdot 7H_2O$; 26.6 g L^{-1} NaCl; 5.4 g L^{-1} $MgCl_2 \cdot 6H_2O$; 1.0 mg L^{-1} resazurin. The pH was adjusted to 7.2 with NaOH under OFN, 30.0 mL L^{-1} of 84.0 g L^{-1} saturated $NaHCO_3$ solution added, and the medium transferred to an anaerobic cabinet (Forma Scientific, UK, gas composition 80% N_2, 10% CO_2, 10% H_2). The medium was dispensed and crimp-sealed (butyl septa) in the anaerobic cabinet and autoclaved. Positive growth in each of the vials was determined by production of a black FeS precipitate.

Methane-oxidizing sulfate-reducing bacteria medium: 0.5 g L^{-1} KH_2PO_4; 1.0 g L^{-1} NH_4Cl; 1.0 g L^{-1} $CaSO_4$; 2.0 g L^{-1} $MgSO_4 \cdot 7H_2O$; 0.1 g L^{-1} yeast extract; 0.1 g L^{-1} ascorbic acid; 0.1 g L^{-1} thioglycollic acid; 0.5 g L^{-1} $FeSO_4 \cdot 7H_2O$; 26.6 g L^{-1} NaCl; 5.4 g L^{-1} $MgCl_2 \cdot 6H_2O$; 1.0 mg L^{-1} resazurin. The pH was adjusted to 7.2 with NaOH under OFN, and 30.0 mL L^{-1} of 84.0 g L^{-1} saturated $NaHCO_3$ solution added. The mixture was transferred to an anaerobic cabinet, and the medium was dispensed, crimp-sealed (butyl septa), and autoclaved. Once injected with diluted sample, the headspace was pressurized to +5 p.s.i. with sterile (0.1-µm filter) methane. Positive growth in each of the vials was determined by increase in headspace CO_2 and decrease in headspace methane in each vial by GC.

Potential Activity Measurements

Injection Schedule

The 5-cm^3 subcores were allowed to equilibrate overnight before injection with radiotracers using a specially designed injection rig (Parkes et al., 1995) that allowed an even distribution of isotopes along the center line of the subcore. Each group of ten subcores was divided into one time-zero control and triplicate samples in each of three incubation periods. Time-zero subcores were prechilled at 4°C, injected and immediately frozen, and stored in anaerobic bags at –20°C. Incubated samples were sealed in anaerobic bags after injection and incubated at the approximate mean downhole temperature of 12°C for varying periods (specified in text below). Incubations were terminated by freezing at –20°C, and subcores were stored frozen prior to analysis. In all cases, time-zero control results were subtracted from experimental data before calculation of potential activity rates.

Potential Methane Oxidation

The ^{14}C methane (supplied by Amersham, U.K.) was removed from an adapted break-seal ampule using a sterile gas syringe. Fifty µL of gas were injected into each subcore. Equivalent volumes of sterile 0.1 M NaOH were added to the gas reservoir to maintain pressure before further removal of gas samples. Methane oxidation rates were determined from the amounts of $^{14}CO_2$ produced during incubation periods varying from 18 hr to 48 days, depending on sample depth. Frozen syringe subcores were ejected into 30-mL serum vials containing 10 mL of 0.6 M NaOH and a small magnetic stirrer. The vial was crimp sealed, shaken vigorously to disperse the sediment, and flushed with OFN at 60 mL min^{-1} for 30 min. The methane content of the vial was then determined after oxidation to $^{14}CO_2$ (Cragg et al., 1995), and once all residual methane had been stripped from the vial it was transferred to a second flushing rig including two acid traps (1 M HCl) to intercept aerosol droplets. The vial contents were acidified (2 mL of 2 M H_2SO_4) and stirred, and the headspace flushed with OFN for 40 min at 80 mL min^{-1}. Labeled CO_2 was trapped in three sequential vials containing scintillation cocktail designed to trap CO_2 (800 mL toluene, 70 mL β-phenylethylamine, 80 mL methanol, 5 g PPO, 0.1 g POPOP, [Cragg et al., 1990]) and ^{14}C activity determined by liquid scintillation counting (LSC, LKB-Wallace 1414).

Potential Methanogenesis from Bicarbonate

Sample subcores were injected with 7.2 µL (4.8 µCi) of sodium ^{14}C-bicarbonate solution (supplied by Amersham UK, diluted with filter-sterilized [0.2 µm], degassed distilled water), and incubated for varying time periods (from 18 hr to 48 days) before termination by freezing. Rates of methanogenesis from bicarbonate were determined from the amount of $^{14}CH_4$ produced, calculating pore-water carbon dioxide from alkalinity data. Frozen subcores were ejected into 10 mL of 0.6 M NaOH in a 30-mL serum vial, which was crimp sealed with a butyl rubber septum. $^{14}CH_4$ was stripped from the vial by flushing with OFN (60 mL min^{-1} for 40 min), oxidized to $^{14}CO_2$, and trapped in β-phenylethylamine scintillation cocktail for LSC as described above.

Potential Sulfate Reduction

Rates of sulfate reduction were determined from the proportion of ^{35}S-labeled sulfide produced. Subcores were injected with 7.2 µL (3.6 µCi) of ^{35}S sodium sulfate solution (Amersham UK, diluted with filter-sterilized [0.2 µm], autoclaved distilled water) and incubated for varying time periods (from 18 hr to 48 days) before termination by freezing.

A sequential distillation regime was used to separate labeled sulfides into three fractions (Allen and Parkes, 1995). Frozen syringe subcores were ejected into 10 mL of 20% (w/v) zinc acetate solution and allowed to thaw with occasional mixing. Subsample aliquots (1 mL) were removed from the thawed samples after vortex mixing and added to a conical flask containing 10 mL of 35‰ NaCl and a magnetic stirrer. The flask was attached to a distillation rig, and the headspace flushed with OFN for 15 min at 80 mL min^{-1} before addition of 2 mL of 6 M HCl. The flasks were heated to 80°C and distilled for 40 min, trapping labeled acid-volatile sulfide in 10 mL of 10% (w/v) zinc acetate. The flasks were then allowed to cool before addition of 5 mL 95% (v/v) ethanol, 25 mL $CrCl_2$ and 5 mL of concentrated HCl. This cold chromous chloride distillation (pyritic sulfide fraction) was allowed to proceed for 40 min, after which the flask was heated to 80°C for a further 40 min of hot chromous chloride distillation (elemental sulfur fraction). At the end of each distillation period the zinc acetate traps were changed and aliquots (1 mL) removed for determination of ^{35}S activity by LSC and total sulfide by spectrophotometry (Cline, 1969). Total reduced inorganic sulfide (TRIS) was calculated as the sum of the three sulfide fractions.

Thymidine Incorporation

Syringe subcores were injected with 25 µL (18 µCi) of *methyl*[^3H]thymidine (83 Ci $mmol^{-1}$, Amersham UK) and incubated for varying time periods (from 30 min to 36 hr) before termination of the incubations by freezing. Frozen samples were transferred to a 13-mL centrifuge tube containing 5 mL of 20% (w/v) aqueous trichloroacetic acid (TCA) solution and allowed to thaw, mixing thoroughly at intervals. Labeled DNA was extracted from the sediment by an acid-base hydrolysis method (Wellsbury et al., 1993; Wellsbury et al., 1994; Wellsbury et al., 1996). Rinsed, dried sediment was hydrolyzed with 1 M NaOH at 37°C for 1 hr, and centrifuged (2500 × *g* for 10 min at 4°C). The supernatant was removed, cooled to 4°C, and DNA reprecipitated by addition of 1.5 mL of 20% (w/v) TCA in 3.6 M HCl, Kieselguhr, and 50 µL of a saturated solution of unlabeled "carrier" DNA. Following centrifugation (2500 × *g* for 10 min at 4°C) and rinsing (once each with 5% (w/v) TCA, 95% (v/v) ethanol, all at 4°C), labeled DNA was extracted from the pellet in 5% TCA at 100°C for 30 min, and activity determined by LSC.

Potential Acetate Turnover

Replicate syringe subcores were injected with 7.4 µL (7.4 µCi) of [1–(2)^{14}C] acetate (Amersham UK) and incubated for varying time periods (from 1 hr to 13 days) before termination by freezing. Frozen subcores were ejected into 30-mL serum vials containing 10 mL of 0.6 M NaOH, crimp sealed with butyl septa, and allowed to thaw before extraction of labeled $^{14}CH_4$ and $^{14}CO_2$ as described above. Rates of methane and carbon dioxide production were calculated based on the proportion of labeled gas produced and the bioavailable pore-water acetate pool determined by HPLC.

Pore-Water Acetate Determination by HPLC

Pore-water acetate concentrations were determined using an enzymatic method (King, 1991). Aliquots (20 µL) of each of (1) bovine serum albumin (BSA, 200 µg mL^{-1}); (2) disodium ATP (10 mM); (3) coenzyme A (sodium salt, from yeast, 10 mM); and (4) acetyl coenzyme A syntheses (20 U mL^{-1}, ~4.9 U mg^{-1} protein) were added to 1 mL thawed pore water in a screw-cap 2.5-mL vial with an integral O-ring seal (Sarstedt, Leicester, UK). The samples were mixed thoroughly and incubated at 37°C for 1 hr before termination by immersion in a boiling water bath for 2 min. After cooling, 800-µL aliquots were transferred to glass autosampler vials and stored in a cooled autos ampler at 4°C before separation by HPLC (Waters UK). Samples (10-µL injections) were injected onto an analytical column (Supelco LC-18-T, 25 cm × 4.6 mm) with a mobile phase of 0.1 M KH_2PO_4 (pH 6.0) at 30°C at 0.8 mL min^{-1}. Detection was by UV/vis detector at 254 nm and quantification by peak-area integration (Waters data module). Deeper samples containing high concentrations were diluted appropriately such that the detector response was ≤100-µM acetate.

RESULTS

Site 994

Bacterial Populations

Bacteria were present in significant numbers in all samples throughout the depth profile (Fig. 2A). Total bacterial populations were highest near the sediment surface (2.50 × 10^9 cells mL^{-1}) and, overall, decreased with depth throughout the core. The bacterial population in the deepest sample (688.4 mbsf), 2.6 × 10^6 cells mL^{-1}, represents a >99.9% decrease of the near-surface population. However, at two points within the depth profile, the trend was reversed and numbers of bacteria significantly increased, at 355.7 ($P < 0.02$) and 439.5 mbsf ($P < 0.001$). The greatest increase of five fold occurred at 439.5 mbsf, the sample corresponding most closely to the assumed position of the BSR (440 ± 10 mbsf). A similar trend occurred in the numbers of dividing and divided cells, which represented, on average, 9.5% of the total bacterial population at Site 994.

Populations of viable sulfate-reducing bacteria decreased rapidly from a near-surface maximum (1.1 × 10^6 cells mL^{-1} at 0.1 mbsf, Fig. 2A) and were not detected below 1.6 mbsf, apart from the deepest sample at 641 mbsf, where a small number of viable cells (2.0 cells mL^{-1}) were present. However, at several points downcore, populations of viable methane-oxidizing, sulfate-reducing bacteria were detected, with maximum numbers coinciding with a peak in headspace methane (26,000 ppmv at 32 mbsf). Viable nitrate-reducing bacteria were present in all samples, in low numbers, showing a uniform depth distribution (data not shown). Fermentative anaerobic heterotrophs were present in high numbers in all the samples, with large numbers of viable cells present near the sediment surface (2.8 × 10^6 cells mL^{-1} at 0.5 mbsf). A significant peak ($P < 0.05$) in viable fermentative heterotroph numbers was present deep in the sediment, at 566 mbsf, where numbers reached 2.6 × 10^7 cells mL^{-1}.

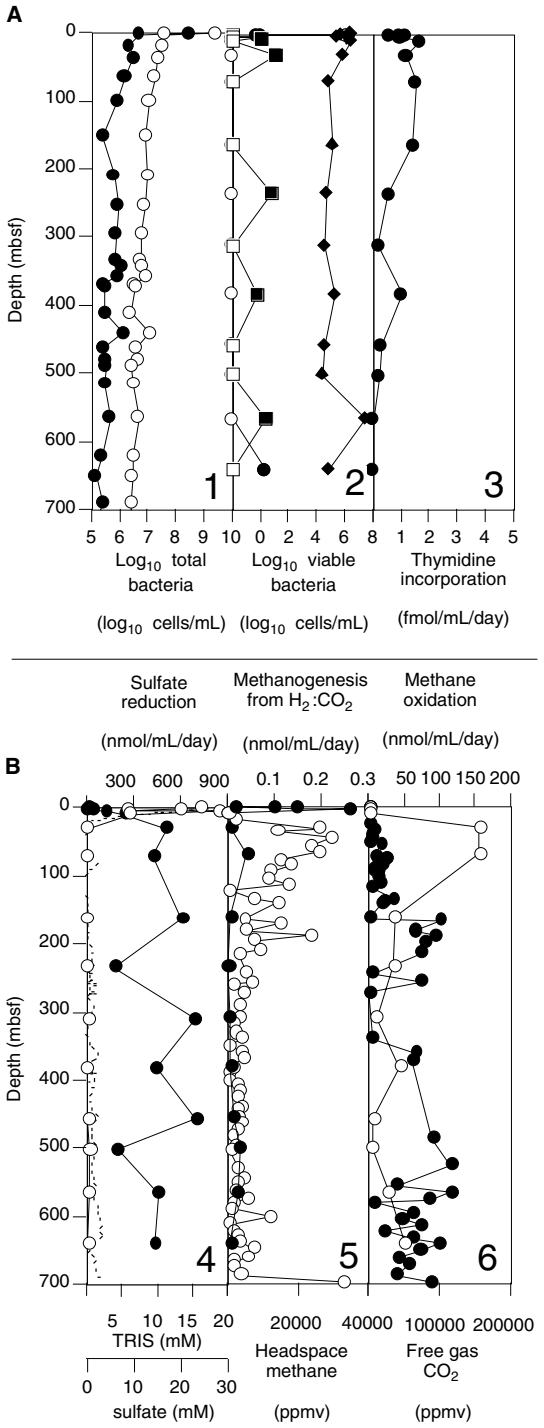

Figure 2. Site 994 bacterial and geochemical depth distributions. **A.** Bacterial populations, viability, and growth. (1) Total bacteria (open circles) and numbers of dividing and divided cells (solid circles). (2) Sulfate-reducing bacteria (circles), fermentative heterotrophs (diamonds), and methane-oxidizing sulfate reducing bacteria (squares). Open symbols indicate that no bacteria were detected. (3) Growth rates estimated by thymidine incorporation (solid circles). **B.** Bacterial activity and associated geochemistry. (4) Potential bacterial sulfate reduction rate (open circles), total reduced inorganic sulfide (TRIS; solid circles), and interstitial water sulfate (dashed line). (5) Potential rate of bacterial methanogenesis from H_2:CO_2 (solid circles) and headspace methane (open circles). (6) Potential bacterial methane oxidation rate (open circles) and headspace carbon dioxide (solid circles).

Rates of bacterial growth, as measured by incorporation of *methyl*[^{3}H]thymidine into DNA, decreased with depth in near-surface sediment from a maximum of 1.14 pmol [mL^{-1} per day] at 0.1 mbsf (Fig. 2A) to 0.55 pmol mL^{-1} per day at 1.6 mbsf. Below this depth, there was a broad, significant ($P < 0.001$) peak in thymidine incorporation rates down to 162 mbsf (1.40 pmol mL^{-1} per day), below which rates decrease, similar to the depth profile of methane oxidation rates. Rates generally decreased with increasing depth below this, although there was a clear peak at 381.4 mbsf (1.00 pmol mL^{-1} per day). Thymidine incorporation rates correlated significantly with microscopically determined numbers of dividing and divided cells at Site 994 ($R = 0.945$, $n = 15$, $P < 0.002$).

Potential Bacterial Activity

During collection and subsequent handling of samples, it is presently impossible to maintain in situ conditions. Although the incubations used for process-rate determinations were carried out at in situ temperatures, facilities do not exist to obtain and subsequently handle samples at in situ pressures. Thus, bacterial activity rates are described as "potential" rates, as they may differ from those in situ.

Bacterial sulfate-reduction rates were high in near-surface sediment (725 nmol mL^{-1} per day at 0.1 mbsf; Fig. 2B), increasing to 842 nmol mL^{-1} per day at 4 mbsf and, although subsequently decreasing with depth, rates were still high to 8.8 mbsf (269 nmol mL^{-1} per day). Below this depth, sulfate-reduction rates were very low (0.8 nmol mL^{-1} per day at 29.8 mbsf), although a 17.5× increase, to 14 nmol mL^{-1} per day, occurred at 500.8 mbsf. The sulfate reduction rate correlated significantly with the interstitial water sulfate concentration ($R = 0.84$; $n = 15$; $P < 0.002$).

Rates of methanogenesis from HCO_3 were low at Site 994: near the sediment surface they were four orders of magnitude lower than sulfate-reduction rates, and generally decreased with increasing depth. A near-surface maximum was present at 4 mbsf (0.26 nmol mL^{-1} per day; Fig. 2B), with further, minor, peaks at 69.3 mbsf (0.041 nmol mL^{-1} per day) and a broader increase to 0.026 nmol mL^{-1} per day between 456.51 and 565.91 mbsf.

Methane-oxidation rates followed a contrasting trend to both sulfate reduction and methanogenesis, increasing from <0.02 nmol mL^{-1} per day in near-surface sediments to a broad peak of ~155 nmol mL^{-1} per day at 29.8 and 69.3 mbsf (Fig. 2B). Rates of methane oxidation then decreased with increasing depth below this peak down to 500 mbsf, although there was an increase to 43 nmol mL^{-1} per day at 381 mbsf. Below 566 mbsf, rates of methane oxidation began to increase with increasing depth.

Pore-Water and Gas Geochemistry

Interstitial water sulfate concentrations at Site 994 decreased rapidly with depth from 25.6 mM at 1.4 mbsf to 1.2 mM at 20 mbsf, consistent with the high near-surface rates of bacterial sulfate reduction (Fig. 2). Below ~60 mbsf, the sulfate profile was irregular, with low concentrations of sulfate (0–0.2 mM) detected.

Sulfide concentrations (TRIS) were low (<0.1 mM) near the sediment surface at Site 994, reflecting oxidative loss at the sediment/water interface (Fig. 2B). Sulfide concentrations increased rapidly with depth, and reached 11 mM by 30 mbsf, reflecting high rates of sulfate reduction.

Headspace methane increased rapidly from 11 to 29,000 ppmv between 9 and 46 mbsf (Fig. 2B), decreasing to ~3000 ppmv by a depth of 310 mbsf. Below 310 mbsf, headspace methane concentrations remained uniform with increasing depth. The C_1/C_2 hydrocarbon ratios indicated that the methane is microbial in origin (Paull, Matsumoto, Wallace, et al., 1996; Schoell, 1980). Concentrations of CO_2 were low near the sediment surface and generally increased with increasing depth (Fig. 2B). These increases are consistent with continued low levels of organic matter oxidation and methane oxidation within the sediments. Total organic carbon (TOC) in the sediments from Site 994 averaged 0.7% in the uppermost 160 mbsf (Paull, Matsumoto, Wallace, et al., 1996). Below 160 mbsf, organic carbon increases to a mean of 1.4%, with a maximum at 612 mbsf.

Site 995

Bacterial Populations

Near-surface bacterial populations were higher at Site 995 than at the other two sites, at 3.39×10^9 cells mL^{-1} (Fig. 3A). Bacteria were present in all samples, and numbers generally decreased from a surface maximum with increasing depth. However, at the BSR (446.2 mbsf), there was a significant peak ($P < 0.01$) where total numbers increased fivefold, from 7.0 to 7.7 log cells mL^{-1}. Similar trends were also evident in the numbers of dividing and divided cells, which comprised, on average, 10.8% of the total population. Again, associated with the BSR was an increase in numbers of cells involved in division, from approximately 1.3×10^6 cells mL^{-1} to 4.4×10^6 cells mL^{-1}. The deepest sample, 700.8 mbsf, contained 4.6×10^6 cells mL^{-1}, 0.13% of the population at the sediment surface.

Viable populations of sulfate-reducing bacteria decreased rapidly with depth from a near-surface maximum (1.1×10^6 cells mL^{-1}). In several samples downcore sulfate-reducing bacteria were not detectable, but around the hydrate zone a small, but consistent population of sulfate-reducing bacteria were present, with a maximum at 439 mbsf, close to the BSR. Below this, sulfate-reducing bacteria were undetectable. Sulfate-reducing bacteria oxidizing methane as a carbon source were also found in low numbers in Site 995, with a near-surface maximum at 0.6 mbsf. Numbers of viable fermentative heterotrophs showed a relatively uniform distribution with depth, although there were distinct peaks both near surface and associated with the BSR. Nitrate-reducing bacteria were only present in low numbers at Site 995, and showed a relatively uniform distribution with depth (data not shown).

Thymidine incorporation rates were highest near the sediment surface (4.1 pmol mL^{-1} per day) and decreased rapidly with depth to zero at 1.7 mbsf. Between 3.8 and 365 mbsf, low rates of thymidine incorporation occurred (0.2–0.7 pmol mL^{-1} per day). In the hydrate zone growth rates increased, reaching a peak at 465 mbsf (1.3 pmol mL^{-1} per day). In situ growth rates, as estimated by thymidine incorporation, correlate significantly with numbers of dividing and divided cells determined by microscopy at Site 995 ($R = 0.67$, $n = 16$, $P < 0.001$).

Potential Bacterial Activity

Sulfate-reduction rates were high in near-surface sediment and decreased rapidly with depth from 400 nmol mL^{-1} per day at 0.1 mbsf to 0.9 nmol mL^{-1} per day at 28.6 mbsf (Fig. 3B). Between 82 and 248 mbsf, no sulfate was detected in pore waters; thus the sulfate-reduction rate was zero. In deep sediment layers, there was an increase in sulfate reduction at, and below, the BSR depth, with a maximum value of 11 nmol mL^{-1} per day in the deepest sample at 691 mbsf. Pore-water sulfate concentrations and numbers of viable sulfate-reducing bacteria both correlated significantly ($P < 0.002$ for both) with measured rates of sulfate reduction.

Rates of methanogenesis from H_2:CO_2 were low in all samples (Fig. 3B). In the uppermost 4 mbsf the rate did not exceed 0.2 nmol mL^{-1} per day, and from 4 to 365 mbsf rates were below 0.04 nmol mL^{-1} per day. In the deep sediment around the hydrate zone there was a clear increase in rates of methanogenesis to 2.7 nmol mL^{-1} per day at 423 mbsf, 27 times the surface rate. This order of magnitude was maintained until 501 mbsf, below which the rate dropped sharply to rates of <0.02 nmol mL^{-1} per day.

In contrast, rates of methanogenesis from acetate (Fig. 3B) were at least two, and up to five orders of magnitude higher than H_2:CO_2 methanogenesis. In the near surface (1.65 mbsf), the rate of acetoclastic methanogenesis peaked at 182 nmol mL^{-1} per day, and then decreased sharply to 0.3 nmol mL^{-1} per day at 3.8 mbsf. A secondary

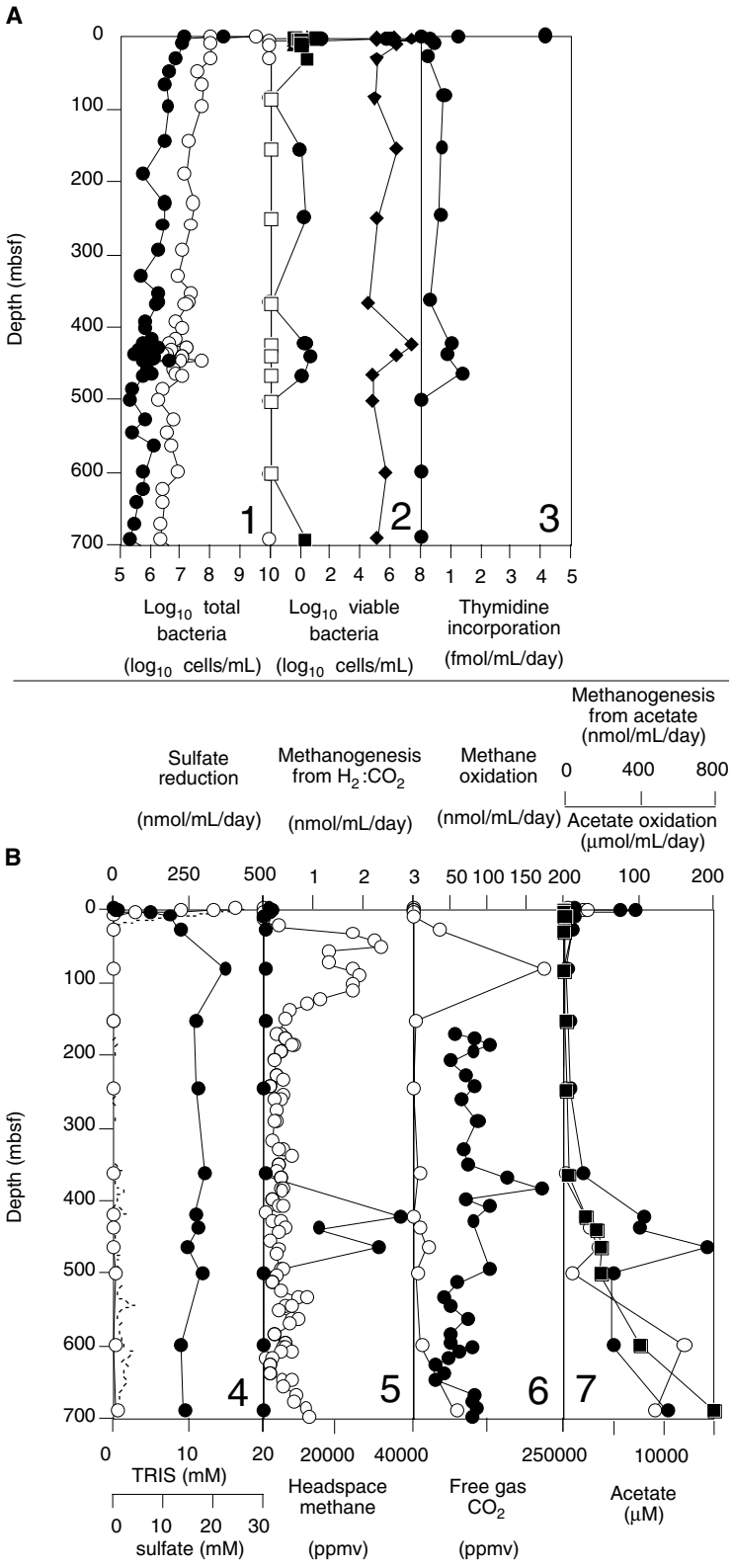

Figure 3. Site 995 bacterial and geochemical depth distributions. **A.** Bacterial populations, viability, and growth. (1) Total bacteria (open circles) and numbers of dividing and divided cells (solid circles). (2) Sulfate reducing bacteria (circles), fermentative heterotrophs (diamonds), and methane-oxidizing sulfate reducing bacteria (squares). Open symbols indicate that no bacteria were detected. (3) Growth rates estimated by thymidine incorporation (solid circles). **B.** Bacterial activity and associated geochemistry. (4) Potential bacterial sulfate reduction rate (open circles), total reduced inorganic sulfide (TRIS; solid circles), and interstitial water sulfate (dashed line). (5) Potential rate of bacterial methanogenesis from H_2:CO_2 (solid circles) and headspace methane (open circles). (6) Potential bacterial methane oxidation rate (open circles) and headspace carbon dioxide (solid circles). (7) Interstitial water acetate concentration (solid squares), potential rates of bacterial methanogenesis from acetate (open circles), and acetate oxidation to carbon dioxide (solid circles).

peak occurred at 29 mbsf (58 nmol mL^{-1} per day), followed by a decrease to <1 nmol mL^{-1} per day at 247 mbsf. At 423 mbsf, there was a 260-fold increase in rates of methane production from acetate, with rates of 209 nmol mL^{-1} per day. Activity continued to increase through the BSR (440 ± 10 mbsf) to a maximum of 340 nmol mL^{-1} per day at 465 mbsf. Below this depth, there was a decrease in the rate of acetoclastic methanogenesis, to 70 nmol mL^{-1} per day at 501 mbsf. However, in contrast to H_2:CO_2 methanogenesis, rates of acetate methanogenesis increased in deeper sediments and reached a maximum of 635 nmol mL^{-1} per day at 600 mbsf.

Rates of acetate turnover to CO_2 were generally high, often three orders of magnitude greater than acetate methanogenesis (Fig. 3B). Near the sediment/water interface, the rate of acetate oxidation reached 94 and 72 µmol mL^{-1} per day at 0.6 and 1.7 mbsf. Below this

rates decreased, remaining reasonably constant until 423 mbsf. Through the hydrate zone there was a significant increase in acetate turnover, with a peak of 190 μmol mL^{-1} per day at 465 mbsf, 15 times the near-surface rate. Below the hydrate zone rates remained significant at ~64 μmol mL^{-1} per day, before a further increase in the deepest sample, 691 mbsf, to 137 μmol mL^{-1} per day.

Methane-oxidation rates were very low (<0.09 nmol mL^{-1} per day) in the uppermost 10 mbsf at Site 995 (Fig. 3B). These rates increased by three orders of magnitude to 34 nmol mL^{-1} per day by 29 mbsf, and reached a maximum of 174 nmol mL^{-1} per day at 82 mbsf, coincident with high concentrations of methane (Fig. 3B). Between 82 and 423 mbsf rates remained generally low, before a peak (19 nmol mL^{-1} per day) around the depth of the BSR, and a further increase in the deepest samples (to 57 nmol mL^{-1} per day at 691 mbsf).

Pore-Water and Gas Geochemistry

Concentrations of pore-water acetate were low in near-surface sediment and remained low (<68 μM) to a depth of 154 mbsf (Fig. 3B). Below this, acetate concentrations begin to increase dramatically, reaching 2198 μM by 423 mbsf, and continued to increase below the hydrate zone. The maximum acetate concentration was in the deepest sample at 691 mbsf, 14,922 μM, an increase of four orders of magnitude from the sediment surface. These results were confirmed by ion-exclusion chromatography (Wellsbury et al., 1997).

Sulfate concentrations at Site 995 decreased rapidly with depth from 26.4 mM at 1.45 mbsf to 2.1 mM at 20.25 mbsf, consistent with the high near-surface rates of bacterial sulfate reduction (Fig. 3B). Below approximately 22 mbsf, the sulfate profile was irregular with low concentrations of sulfate (0–0.2 mM) detected. Concentrations of sulfides were low (<0.5 mM) near the sediment surface at Site 994, reflecting oxidative loss at the sediment/water interface (Fig. 2B). Sulfide concentrations increased rapidly with depth, and reached 8.1 mM by 28.6 mbsf, reflecting high rates of sulfate reduction.

Sediment TOC was generally below 1% in the uppermost 119 mbsf at Site 995, averaging 0.72% (Paull, Matsumoto, Wallace, et al., 1996). Deeper in the sediment, TOC increased to an average of 1.32%, with uniform depth distribution.

Headspace methane increased from 3.2 to 31,000 ppmv between 0 and 52 mbsf (Fig. 3B), and subsequently decreased to ~<5000 ppmv by 171 mbsf. Between 171 and 514 mbsf, headspace methane concentrations remained uniform with increasing depth. Between 514 and 608 mbsf, there was a zone containing two maxima (11,500 and 9000 ppmv at 533 and 563 mbsf respectively). Below 608 mbsf, headspace methane concentrations increased with depth, and reached 12,200 ppmv in the deepest sample, 699 mbsf.

The CO_2 concentrations were relatively uniform with depth (Fig. 3B), although there were peaks within the profile, consistent with deep bacterial activity. Below 650 mbsf, for example, increasing CO_2 concentrations coincided with an increase in the rate of methane oxidation.

Site 997

Bacterial Populations

Bacteria were present in all samples to a depth of 748.49 mbsf (Fig. 4A). Total bacterial populations decreased rapidly from a near-surface maximum (2.42×10^9 cells mL^{-1} at 0.025 mbsf). Substantial numbers remained even at 748 mbsf (1.8×10^6 cells mL^{-1}), however, despite the 99.9% decrease in population size. Above this decreasing trend with depth there were some increases in bacterial numbers, notably at 310–331 mbsf, with a peak (2.13×10^7 cells mL^{-1}) at 331 mbsf, the depth from which a "massive" methane hydrate deposit was recovered (Paull, Matsumoto, Wallace, et al., 1996). A further, significant ($P < 0.002$) increase in bacterial populations at 451–473 mbsf was associated with the BSR, with a 19-fold increase at 451 mbsf and an associated maximum at 469 mbsf (2.43×10^7 cells mL^{-1}). In the depth interval between 338 and 443 mbsf, a zone of relatively low bacterial numbers occurred, bounded by the "massive" hydrate deposit and the BSR and free-gas zone. However, within this interval there was an increase (of one order of magnitude) at 388 mbsf, which coincides with a substantial deep subsurface peak in headspace methane (Fig. 4B). The depth distribution of dividing and divided cells was similar to that of the total bacterial population (Fig. 4A) and represented, on average, 13.1% of the total population. Clear increases in the numbers of cells involved in division were associated with both the "massive" hydrate deposit (331 mbsf) and the BSR.

Only six WRC samples were taken at Site 997, spanning the interval 331–469 mbsf. Small numbers of viable sulfate-reducing bacteria were present in all six samples, with a small increase at 444 mbsf associated with the BSR (Fig. 4B). Viable methane-oxidizing, sulfate-reducing bacteria were only detected in the 444-mbsf sample, close to the BSR, and in very low numbers (1.0×10^1 cells mL^{-1}). Nitrate-reducing bacteria were present in all samples, with a uniform depth distribution (data not shown). Fermentative heterotrophic bacteria were present in all samples, with the greatest numbers at 331 and 492 mbsf (2.9×10^6 cells mL^{-1}) and a minimum at 451 mbsf (9.8×10^4 cells mL^{-1}).

Thymidine incorporation rates were low (Fig. 4A) even compared to the same depths at the other sites, ranging from zero to 0.2 pmol mL^{-1} per day. Maximal growth rates were present at 372 and 492 mbsf, with rates at the other depths at or near the detection limit.

Potential Bacterial Activity

Sulfate-reduction rates were low (<0.1 nmol mL^{-1} per day) between 331 and 372 mbsf, although similar to rates at similar depths at the other sites. Below this, rates were generally an order of magnitude higher (range 0.2–1.0 nmol mL^{-1} per day) and there was a clear peak at 451 mbsf (2.2 nmol mL^{-1} per day) associated with the BSR. Rates of bacterial sulfate reduction correlate significantly with pore-water sulfate concentrations ($R = 0.84$, $n = 6$, $P < 0.05$).

Rates of H_2:CO_2 methanogenesis in the six deep samples were highest from 331 to 372 mbsf, where the maximum rate was 5.6 nmol mL^{-1} per day (Fig. 4B). Below 372 mbsf, rates were relatively low (<0.5 nmol mL^{-1} per day), with a minimum (0.02 nmol mL^{-1} per day) at 451 mbsf.

A clear maximum rate of anaerobic bacterial methane oxidation was measured at 416 mbsf (109 nmol mL^{-1} per day). In the remaining deep samples, methane oxidation rates were generally in the range 4–14 nmol mL^{-1} per day, although rates again increased to 61 nmol mL^{-1} per day in the deepest sample analyzed (492 mbsf).

Pore-Water and Gas Geochemistry

Interstitial water sulfate concentrations decreased rapidly within the uppermost ~20 m of sediment, from 26.8 mM at 1.45 mbsf to 1.5 mM at 21.3 mbsf (Fig. 4B). As at the two other sites, below this the sulfate concentration remained low, with small increases in deep sediment, which may reflect either contamination or a source of sulfate. Sulfide was present in all samples from Site 997 in higher concentrations than at similar depths at the other two sites, ranging from 11.5 to 20.6 mM between 331 and 491 mbsf. A maximum (20.6 mM) was detected at 444 mbsf, close to the position of the BSR.

Sediment TOC was generally below 1% in the uppermost 96 mbsf at Site 995, averaging 0.82% (Paull, Matsumoto, Wallace, et al., 1996). Deeper in the sediment, TOC increased to an average of 1.38%, with uniform depth distribution. Gas samples taken at Site 997 showed some irregularities because of air contamination during sampling (Paull, Matsumoto, Wallace, et al., 1996). Headspace methane increased from 3.2 to 56,200 ppmv between 0 and 50.4 mbsf (Fig. 4B), and subsequently decreased to ~ <5000 ppmv by 149 mbsf. Be-

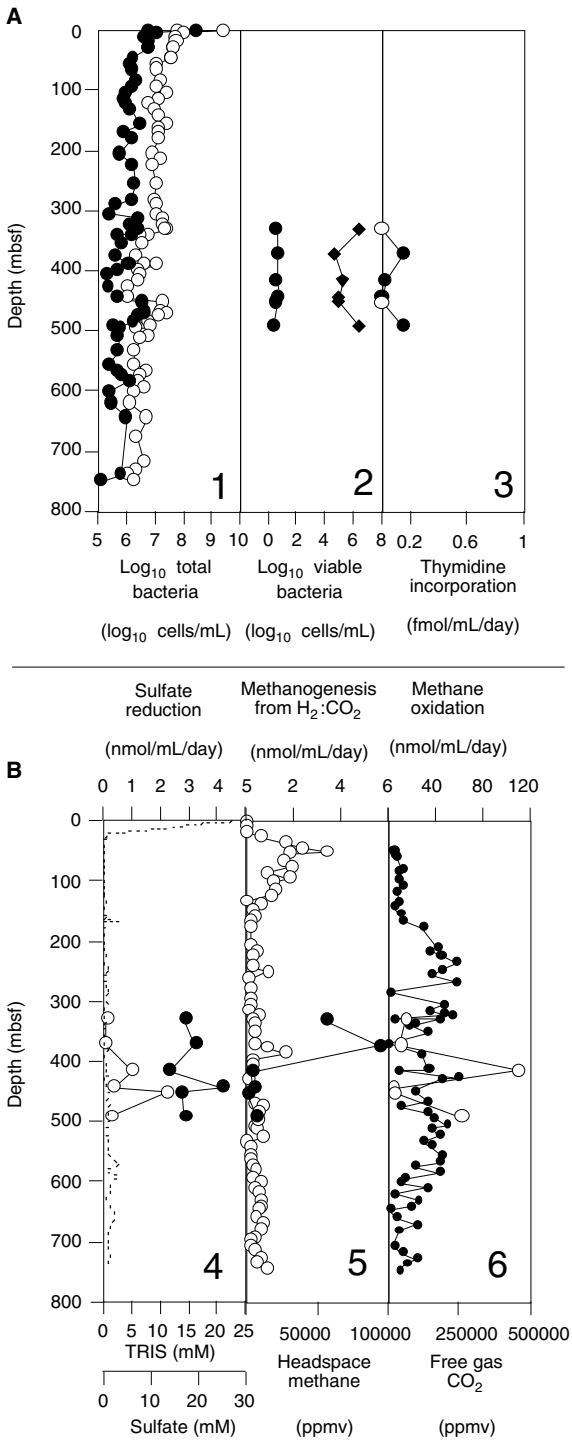

Figure 4. Site 997 bacterial and geochemical depth distribution. **A.** Bacterial populations, viability, and growth. (1) Total bacteria (open circles) and numbers of dividing and divided cells (solid circles). (2) Sulfate reducing bacteria (circles) and fermentative heterotrophs (diamonds). Open symbols indicate that no bacteria were detected. (3) Growth rates estimated by thymidine incorporation (solid circles). **B.** Bacterial activity and associated geochemistry. (4) Potential bacterial sulfate reduction rate (open circles), total reduced inorganic sulfide (TRIS; solid circles), and interstitial water sulfate (dashed line). (5) Potential rate of bacterial methanogenesis from H_2:CO_2 (solid circles) and headspace methane (open circles). (6) Potential bacterial methane oxidation rate (open circles) and headspace carbon dioxide (solid circles).

low this, the concentrations were uniform with depth, with a high degree of scatter. Concentrations of CO_2 broadly increased and then decreased with depth, with a large amount of scatter (Fig. 4B). Within the profile there was a degree of consistency with deep bacterial activity, and particularly methane oxidation (Fig. 4B), with a minimum in both headspace CO_2 and bacterial methane oxidation at 372 mbsf, and a maximum at 416 mbsf.

DISCUSSION

Bacterial Biomass and Productivity

Previous analysis of bacterial distributions in deep sediment samples from six ODP legs in the Pacific (Parkes et al., 1994) and the Atlantic Oceans (Cragg et al., 1997) has demonstrated an exponential relationship between bacterial populations and sediment depth. The consistent bacterial/depth relationship found at other sites with widely differing oceanographic settings suggests that the deep bacterial biosphere is ubiquitous in marine sediments. This relationship also allows comparison with and interpretation of bacterial population data in more complex environments, for example, the sediment at Cascadia Margin (ODP Leg 146; Cragg et al., 1995), where tectonic activity results in the expulsion of large quantities of fluids and volatiles throughout the sediments, and the formation of gas hydrates in some areas.

The total bacterial populations in Leg 164 sediments are consistent with all previous ODP data (Fig. 5). Below ~10 mbsf, however, numbers are comparatively high, and often exceed the upper 95% prediction limit. Bacterial populations are particularly stimulated around the BSR (Fig. 5).

Organic carbon concentrations increased with depth in Leg 164 sediments. Consequently, there is no correlation between organic carbon and the total bacterial population at any of the three sites. Elevated organic carbon at depth may, however, contribute to higher bacterial numbers in the deeper layers of Blake Ridge sediments compared to other ODP sites previously analyzed (Fig. 5).

The deepest marine sediment samples previously examined for bacterial populations were from ODP Leg 161 (Alboran Sea), at a depth of 647 mbsf (Cragg et al., in press). This study extends the depth of known biosphere in marine sediments by a further ~100 mbsf; the deepest sample collected during Leg 164, from 749 mbsf at Site 997, represents the deepest marine sediment sample collected and examined as part of a continuous depth sequence for bacterial populations to date. Even at this depth, the bacterial population at Blake Ridge is substantial, at 1.8×10^6 cells mL^{-1}.

With increasing amounts of hydrate at the three sites (Table 1) and the associated increases in free gas (Dickens et al., 1997), the relative number of cells involved in division increases. The frequency of dividing and divided cells increases from 9.5% at Site 994, through 10.8% at Site 995 to 13.1% at Site 997. This suggests that the presence of the hydrate/free-gas accumulations stimulates bacterial growth and is confirmed by increases in depth-integrated bacterial productivity (thymidine incorporation), which increases from 33 pmol m^{-2} per day at Site 994 to 198 pmol m^{-2} per day at Site 995 within the inferred hydrate zone (a complete data set for thymidine incorporation rates is unavailable for Site 997). Although thymidine incorporation is a reliable index of bacterial productivity in sediments (Wellsbury et al., 1996), conversion into absolute growth rates (Moriarty, 1990) is problematical (Robarts and Zohary, 1993; Wellsbury et al., 1993), and hence growth rates have not been calculated.

The total bacterial population increase, which occurs immediately below the inferred hydrate zone (Fig. 6), is associated with the zone of free gas trapped beneath the "frozen" hydrate (Dickens et al., 1997). Below the inferred hydrate zone, the population increases are such that total bacterial numbers are significantly higher than those immediately above the BSR ($P < 0.005$ and $P < 0.002$ at Sites 995 and

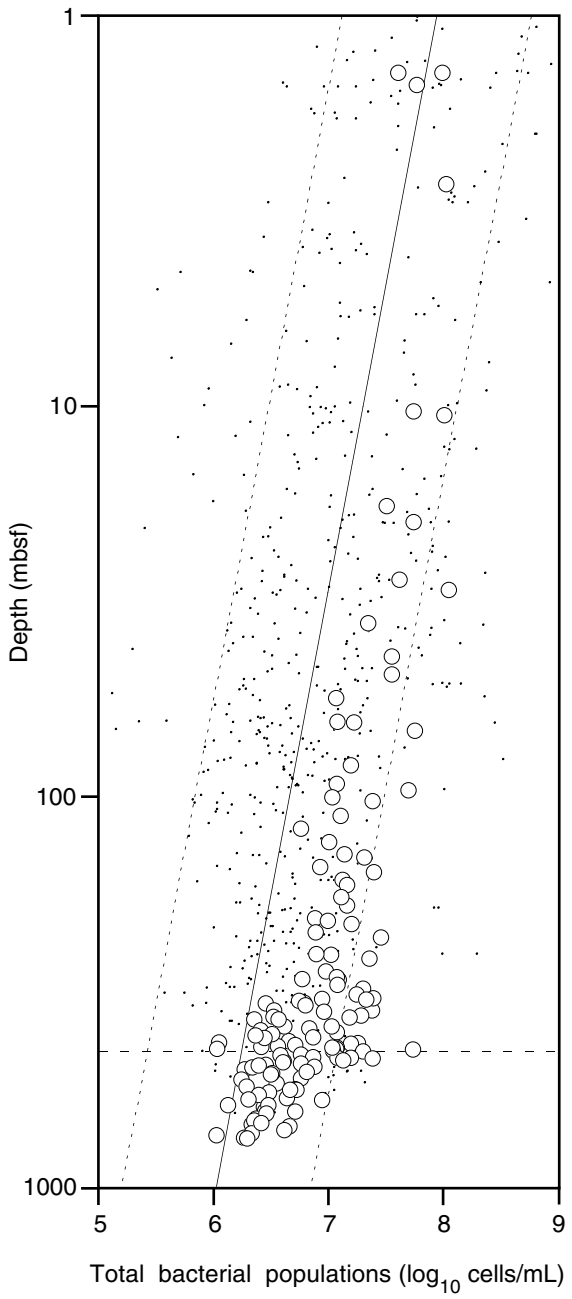

Figure 5. Bacterial populations in all deep marine sediments analyzed to date (small dots) with populations from Sites 994, 995, and 997 overlaid (open circles). The slanting solid line represents the general trend in all sediments ($\log_{10}$ bacterial numbers = 7.95–0.64 $\log_{10}$ depth [m]), and the dashed lines indicate the upper and lower 95% prediction limits. The approximate position of the BSR is represented by the horizontal dashed line.

997). Thus, the population increases suggest an increased biological availability of methane within the free-gas zone.

Total bacterial populations in the samples of solid hydrate recovered from Site 997 (331 mbsf) were much lower than those predicted from a general regression of total populations and depth at Leg 164 sites, as it contained only 2.1% of the expected bacterial population. Thus, solid gas hydrate might physically exclude bacteria, or be colonized by limited numbers of specialized bacteria. Hence, increases and variable distributions in bacterial populations within the inferred hydrate zone (Site 995, 428 mbsf; Fig. 6) probably reflect the patchy distribution of solid hydrate and localized higher free gas concentrations that bacteria can utilize, similar to the situation just below the BSR.

Table 1. Inferred amounts and distributions of gas hydrate in sediments from Leg 164, based on interstitial water chloride anomalies, temperature anomalies in the recovered cores, and patterns in the downhole log data.

Site	Depth interval (mbsf)	Typical amount of gas hydrate (vol%)	Maximum amount of hydrate (vol%)
994	220-430	1.0-3.0	9.5
995	195-440	1.0-4.0	10.0
997	195-450	>1.5-4.0	11.0

Biogeochemical Cycling

In near-surface sediments at Blake Ridge, carbon flow is dominated by bacterial sulfate reduction (Figs. 2B, 3B), which occurs at rates up to four orders of magnitude higher than methanogenesis. Increasing sulfide concentrations (TRIS) and the rapidly decreasing interstitial water sulfate concentrations are both independent confirmations of sulfate reduction. In addition, depth distributions of viable populations of sulfate-reducing bacteria in near-surface Leg 164 sediments reflect this trend (Figs. 2A, 3A). Below ~20 mbsf, pore-water sulfate concentrations are depleted to values of <0.2 mM. Associated with this decrease is an increase in headspace methane, exceeding ~20,000 ppmv by depths of ~30 mbsf. As methane gas increases, so the rates of bacterial methane oxidation increase (to ~160 nmol mL^{-1} per day). Rates of methanogenesis also increase deeper in the sediment (Figs. 2B, 3B)

Potential rates of bacterial activity increase sharply around the base of the inferred hydrate zone and the free-gas zone beneath (e.g., Site 995, Fig. 7). Anaerobic methane oxidation, methanogenesis from both acetate and H_2:CO_2, acetate oxidation, sulfate reduction, and thymidine incorporation are all stimulated. These data clearly demonstrate that the sediments near and below the BSR form a biogeochemically dynamic zone, with carbon cycling occurring through methane, acetate, and carbon dioxide.

In sediments from Cascadia Margin, ODP Leg 146, increasing amounts of hydrate within the sediments resulted in increasing rates of anaerobic methane oxidation (Cragg et al., 1996; Cragg et al., 1995). At Blake Ridge, the largest quantities of hydrate and associated free gas were present at Site 997. Anaerobic methane oxidation rates in the "hydrate zone" at Site 997 reached a maximum of 109 nmol mL^{-1} per day, compared to a maximum of 19 nmol mL^{-1} per day at Site 995. Methane oxidation rates are clearly stimulated in the free-gas zone below the BSR (Fig. 7); thus, increasing amounts of free gas associated with increasing amounts of hydrate impact on methane oxidation rates. These data are in good agreement with the increases in bacterial populations directly within the free-gas zone (Fig. 6) and further substantiate the hypothesis that it is the presence of the free gas associated with the hydrate deposits, rather than the hydrates themselves, that impacts on microbial activity.

Sulfate-reducing bacteria have been implicated in anaerobic methane oxidation (Iversen and Jørgensen, 1985; Schulz, et al., 1994). Both sulfate reduction and methane oxidation were stimulated below the BSR (Fig. 7), but these processes are not closely correlated. The presence of deep interstitial water sulfate may be an indicator of seawater contamination during drilling (Paull, Matsumoto, Wallace, et al., 1996). However, anoxic sulfide oxidation could also produce sulfate (Bottrell et al., unpubl. data; Fossing and Jørgensen, 1990; Schulz et al., 1994). The electron acceptor(s) for this oxidation and methane oxidation might be supplied by fluid flow into the hydrate

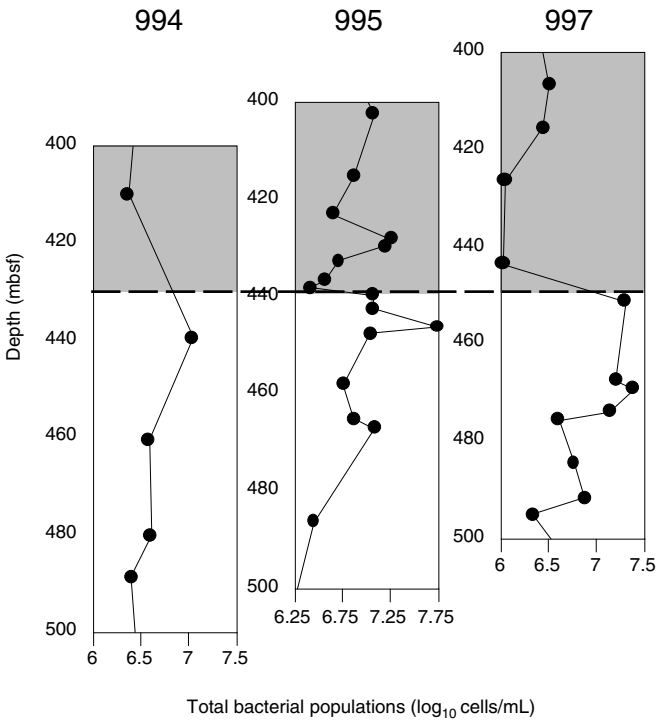

Figure 6. Stimulation of bacterial populations associated with the base of the inferred hydrate zone and free gas beneath. The gray area indicates the inferred hydrate zone at the three sites, and the dashed line emphasizes the boundary with the free gas.

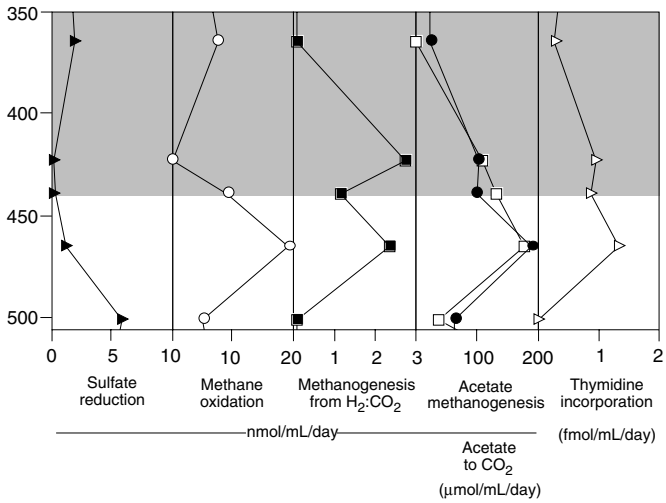

Figure 7. Bacterial activities near the BSR at Site 995. Sulfate reduction (solid triangles), methane oxidation (open circles), methanogenesis from H_2:CO_2 (solid squares), methanogenesis from acetate (open squares), acetate oxidation to CO_2 (solid circles), and bacterial growth rates indexed with thymidine incorporation (open triangles) are shown. The shaded area at 440 mbsf and above indicates the zone where the presence of hydrate was inferred.

zone (P.K. Egeberg, pers. comm., 1998). In addition, other electron acceptors such as ferric iron and humic acids may also be important (Lovley et al., 1996).

The extraordinary depth profile of pore-water acetate at Site 995 (Fig. 3) demonstrates the importance of acetate in biogeochemical cycling in deep marine sediments (Fig. 7). Concentrations of acetate were surprisingly high, reaching ~15 mM at 691 mbsf, ~1000 times higher than "typical" near-surface concentrations. These values were determined by the use of two different, independent analytical techniques. The specific enzymatic HPLC technique was used (ion-exclusion chromatography) and independently confirmed using isotachophoresis on interstitial water samples from Site 997 (Wellsbury et al., 1997).

Rates of potential acetate metabolism in Site 995 sediment are extremely high, reflecting the very high pool size in the interstitial water. Actual turnover rates of labeled [1-(2)^{14}C] acetate, however, were comparatively small (<0.4%/hr below 28 mbsf), so when multiplied by the large pool size this would result in an amplification of any ^{14}C counting errors, which might result in some overestimates of turnover rates. Despite this possibility, acetate turnover is so large that it must be a major energy source for deep sediment bacteria, and consistent with this, the rate of labeled acetate turnover to methane, which is independent of the acetate pool size, increases in the deeper sections (e.g., rates of turnover of labeled acetate to methane increase by 85× between 500 and 600 mbsf). However, as the acetate concentration increases with depth, this means that acetate production must exceed consumption, and thus there must be a significant source of acetate within the deeper zones of both Site 995 and Site 997. Some of this acetate may be produced in situ, as demonstrated by Wellsbury et al. (1997), because temperature increases during burial will increase the bioavailability of organic matter. The increasing acetate concentrations are accompanied by increasing concentrations of other volatile fatty acids (e.g., formate, lactate and propionate [data not shown]) and are consistent with increasing concentrations of dissolved organic carbon at depth in Blake Ridge sediments (Egeberg and Barth, 1998). However, these rates of acetate metabolism are extremely high, and could not be sustained without influx of organic carbon into the sediment; hence in situ rates are likely to be lower than these potential rate measurements. However, Egeberg and Barth (1998) suggest that high dissolved organic carbon is supplied at Site 997 by upward migration of pore water, contributing significantly to the pool of metabolizable carbon. These increases in volatile organic acids may be specific to gas hydrate sites, explaining the high quantities of biogenic methane in the sediments.

Rates of acetate methanogenesis below the BSR are two to three orders of magnitude higher than H_2:CO_2 methanogenesis. Methane oxidation rates at the base of the hydrate zone at Site 995 are 10 times greater than H_2:CO_2 methanogenesis, similar to previous results from Leg 146, where methane oxidation also exceeded methanogenesis (from H_2:CO_2). In contrast, acetate methanogenesis at Site 995 exceeds methane oxidation through and below the BSR, which is consistent with high accumulations of methane below the BSR (Dickens et al., 1997).

SUMMARY

During Leg 146, bacterial numbers and activity rates were found to be stimulated by the presence of a discrete gas hydrate zone in samples from Site 889/890 (Cragg et al., 1995). The data presented here from Leg 164 confirm that the presence of gas hydrate stimulates bacterial populations and activity. These increases within the gas hydrate–stability zone seem to be associated with the presence of free gas within the hydrate deposits rather than the solid hydrate. Bacterial populations in solid hydrate are much lower than in the surrounding sediment. In the free-gas zone immediately below the BSR, there are increases of an order of magnitude in bacterial numbers. Similarly, a range of potential bacterial activities increase around and

below the BSR, suggesting that the free gas associated with the hydrate is an important factor in this stimulation.

Microbiological data from the Blake Ridge sites, and those collected during Leg 146 (Cragg et al., 1995), clearly demonstrate that gas hydrate systems are more biogeochemically dynamic than previously thought. In particular, the high acetate concentrations occurring through and beneath the base of the gas hydrate zone provide an unexpected source of methane gas for the formation of hydrates. The thousand-fold increase in potential rates of acetate methanogenesis (rather than H_2:CO_2) associated with high interstitial water acetate concentrations emphasizes this and, when combined with intense rates of methane oxidation associated with, and beneath the BSR, highlights the role of carbon cycling in these sediments. This, in turn, fuels a thriving bacterial population at depth, reflected by increases in bacterial numbers, numbers of dividing and divided cells, and productivity.

Thus, there is the exciting potential for an increasing bacterial biosphere at depth in gas hydrate–bearing sediments. Both bacterial activity and populations actually increase around and beneath the base of the gas hydrate–stability zone. Previous estimates of the extent of a deep bacterial biosphere in marine sediments, 10% of the surface biosphere in terms of organic carbon (Parkes et al., 1994), were based on a model in which bacterial numbers continued to decrease exponentially with increasing depth. Increasing bacterial activity and populations at depth such as found at Blake Ridge and Cascadia Margin hydrate sediments will increase significantly this estimate of deep bacterial biomass because hydrate-containing sediments are widespread (Kvenvolden, 1988) and contain a significant amount of global fossil fuel carbon.

ACKNOWLEDGMENTS

We wish to thank ODP for allowing us to obtain samples on Leg 164, and particularly the technical staff for their assistance with obtaining the samples. We are grateful to Alistair Lawson, Ian Mather, Sam Bradbrook, and Steve Barnes for their contribution during initial sediment handling in the laboratory. We would like to thank F.S. Colwell and C.K. Paull for their constructive comments on the manuscript. This work was funded by the Natural Environment Research Council (UK) grant GST/02/1239.

REFERENCES

Allen, R.E., and Parkes, R.J., 1995. Digestion procedures for determining reduced sulfur species in bacterial cultures and in ancient and recent sediments. *ACS Symp. Ser.,* 612:243–247.

Brooks, J.M., Bernard, L.A., Weisenburg, D.A., Kennicutt, M.C., II, and Kvenvolden, K.A., 1983. Molecular and isotopic compositions of hydrocarbons at Site 533, Deep Sea Drilling Project Leg 76. *In* Sheridan, R.E., Gradstein, F.M., et al., *Init. Repts. DSDP,* 76: Washington (U.S. Govt. Printing Office), 377–389.

Cline, J.D., 1969. Sectrophotometric determination of hydrogen sulfide in natural waters. *Limnol. Oceanogr.,* 14:454–458.

Cragg, B.A., Bale, S.J., and Parkes, R.J., 1992. A novel method for the transport and long–term storage of cultures and samples in an anaerobic atmosphere. *Lett. Appl. Microbiol.,* 15:125–128.

Cragg, B.A., Law, K.M., Cramp, A., and Parkes, R.J., 1997. Bacterial profiles in Amazon Fan sediments, Sites 934 and 940). *In* Flood, R.D., Piper, D.J.W., Klaus, A., and Peterson, L.C. (Eds.), *Proc. ODP, Sci. Results,* 155: College Station, TX (Ocean Drilling Program), 565–571.

Cragg, B.A., Law, K.M., O'Sullivan, G.M., and Parkes, R.J., in press. Bacterial profiles in deep sediments of the Alboran Sea, Western Mediterranean (Sites 976–978). *In* Zahn, R., Comas, M.C., Klaus, A., and Cita-Sironi, M.-B. (Eds.), *Proc. ODP, Sci Res.,* 161: College Station, TX (Ocean Drilling Program).

Cragg, B.A., and Parkes, R.J., 1994. Bacterial profiles in hydrothermally active deep sediment layers from Middle Valley (NE Pacific), Sites 857 and 858. *In* Mottl, M.J., Davis, E.E., Fisher, A.T., and Slack, J.F. (Eds.), *Proc. ODP, Sci. Results,* 139: College Station, TX (Ocean Drilling Program), 509–516.

Cragg, B.A., Parkes, R.J., Fry, J.C., Herbert, R.A., Wimpenny, J.W.T., and Getliff, J.M., 1990. Bacterial biomass and activity profiles within deep sediment layers. *In* Suess, E., von Huene, R., et al., *Proc. ODP, Sci. Results,* 112: College Station, TX (Ocean Drilling Program), 607–619.

Cragg, B.A., Parkes, R.J., Fry, J.C., Weightman, A.J., Rochelle, P.A., and Maxwell, J.R., 1996. Bacterial populations and processes in sediments containing gas hydrates (ODP Leg 146: Cascadia Margin). *Earth Planet. Sci. Lett.,* 139:497–507.

Cragg, B.A., Parkes, R.J., Fry, J.C., Weightman, A.J., Rochelle, P.A., Maxwell, J.R., Kastner, M., Hovland, M., Whiticar, M.J., and Sample, J.C., 1995. The impact of fluid and gas venting on bacterial populations and processes in sediments from the Cascadia Margin accretionary system (Sites 888–892) and the geochemical consequences. *In* Carson, B., Westbrook, G.K., Musgrave, R.J., and Suess, E. (Eds.), *Proc. ODP, Sci. Results,* 146 (Pt 1): College Station, TX (Ocean Drilling Program), 399–411.

Dickens, G.R., Paull, C.K., Wallace, P., and the ODP Leg 164 Scientific Party, 1997. Direct measurement of in situ methane quantities in a large gas-hydrate reservoir. *Nature,* 385:427–428.

Egeberg, P.K., and Barth, T., 1998. Contribution of dissolved organic species to the carbon and energy budgets of hydrate bearing deep sea sediments (Ocean Drilling Program Site 997 Blake Ridge). *Chem. Geol.,* 149:25–35

Fossing, H., and Jørgensen, B.B., 1990. Oxidation and reduction of radiolabeled inorganic sulphur compounds in an estuarine sediment, Kysing Fjord, Denmark. *Geochim. Cosmochim. Acta,* 54:2731–2742.

Fry, J.C., 1988. Determination of biomass. *In* Austin, B. (Ed.), *Methods in Aquatic Bacteriology:* Chichester (Wiley), 27–72.

————, 1990. Direct methods and biomass estimation. *Meth. Microbiol.,* 22:41–85.

Galimov, E.M., and Kvenvolden, K.A., 1983. Concentrations of carbon isotopic compositions of CH_4 and CO_2 in gas from sediments of the Blake Outer Ridge, Deep Sea Drilling Project Leg 76. *In* Sheridan R.E., Gradstein, F.M., et al., *Init. Repts. DSDP,* 76: Washington (U.S. Govt. Printing Office), 403–407.

Hurley, M.A., and Roscoe, M.E., 1983. Automated statistical analysis of microbial enumeration by dilution series. *J. Appl. Bacteriol.,* 55:159–164.

Iversen, N., and Jørgensen, B.B., 1985. Anaerobic methane oxidation rates at the sulfate-methane transition in marine sediments from Kattegat and Skagerrak (Denmark). *Limnol. Oceanogr.,* 30:944–955.

King, G.M., 1991. Measurement of acetate concentrations in marine pore water by using an enzymatic approach. *Appl. Environ. Microbiol.,* 57:3476–3481.

Kvenvolden, K.A., 1988. Methane hydrate—a major reservoir of carbon in the shallow geosphere? *Chem. Geol.,* 71:41–51.

Lovley, D.R., Coates, J.D., Blunt-Harris, E.L., Phillips, E.J.P., and Woodward, J.C., 1996. Humic substances as electron acceptors for microbial respiration. *Nature,* 382:445–448.

Moriarty, D.J.W., 1990. Techniques for estimating bacterial growth rates and production of biomass in aquatic environments. *Meth. Microbiol.,* 22:211–233.

Parkes, R.J., Cragg, B.A., Bale, S.J., Getliff, J.M., Goodman, K., Rochelle, P.A., Fry, J.C., Weightman, A.J., and Harvey, S.M., 1994. A deep bacterial biosphere in Pacific Ocean sediments. *Nature,* 371:410–413.

Parkes, R. J., Cragg, B. A., Bale, S. J., Goodman, K. and Fry, J. C., 1995. A combined ecological and physiological approach to studying sulphate reduction within deep marine sediment layers. *J. Microbiol. Methods,* 23:235–249.

Paull, C.K., Matsumoto, R., Wallace, P.J., et al., 1996. *Proc. ODP, Init. Repts.,* 164: College Station, TX (Ocean Drilling Program).

Robarts, R.D., and Zohary, T., 1993. Fact or fiction: bacterial growth rates and production as determined by [*methyl*-3H]thymidine? *Adv. Microb. Ecol.,* 13:371–425.

Schoell, M., 1980. The hydrogen and carbon isotopic composition of methane from natural gases of various origins. *Geochim. Cosmochim. Acta,* 44:649–661.

Schulz, H.D., Dahmke, A., Schinzel, U., Wallmann, K., and Zabel, M., 1994. Early diagenetic processes, fluxes, and reaction rates in sediments of the South Atlantic. *Geochim. Cosmochim. Acta,* 58:2041–2060.

Wellsbury, P., Goodman, K., Barth, T., Cragg, B.A., Barnes, S.P., and Parkes, R.J., 1997. Deep marine biosphere fueled by increasing organic matter availability during burial and heating. *Nature,* 388:573–576.

Wellsbury, P., Herbert, R.A., and Parkes, R.J., 1993. Incorporation of *methyl*[^{3}H]thymidine by obligate and facultative anaerobic bacteria when grown under defined culture conditions. *FEMS Microbiol. Ecol.,* 87–95.

————, 1994. Bacterial [*methyl*-H]thymidine incorporation in substrate-amended estuarine sediment slurries. *FEMS Microbiol. Ecol.,* 15:237–248.

————, 1996. Bacterial activity and production in near-surface estuarine and freshwater sediments. *FEMS Microbiol. Ecol.,* 19:203–214.

Date of initial receipt: 27 April 1998
Date of acceptance: 10 March 1999
Ms 164SR-216